ORIGINAL PAPER

CFD SIMULATIONS FOR THE SELECTION OF AN APPROPRIATE BLADE PROFILE FOR IMPROVING ENERGY EFFICIENCY IN AXIAL FLOW MINE VENTILATION FANS

Durga Charan Panigrahi[1] and Devi Prasad Mishra[2]

[1] *Indian School of Mines (Dhanbad, Jharkhand, India)*

[2] *Department of Mining Engineering, Indian School of Mines (Dhanbad, Jharkhand, India)*

Corresponding author: e-mail: devi_agl@yahoo.com, tel.: +91 9430191673; fax: +91 326 2296628/2296563

ABSTRACT

Purpose	This study focuses on one of the key design aspects of mine ventilation fans, i.e. the selection of an appropriate aerofoil blade profile for the fan blades in order to enhance the energy efficiency of axial flow mine ventilation fans, using CFD simulations.
Methods	Computational simulations were performed on six selected typical aerofoil sections using CFD code ANSYS Fluent 6.3.26 at angles of attack varying from 0° to 21° at an interval of 3° and at Reynolds number $Re = 3 \times 10^6$, and various aerodynamic parameters, viz. coefficients of lift (C_l) and drag (C_d) as a function of angle of attack (α) were determined to assess the efficiency of the aerofoils.
Results	The study revealed that the angle of attack has a significant effect on the lift and drag coefficients and stall condition occurred at α values of 12° and 15° in most of the aerofoils. Based on the criterion of higher lift to drag ratio (C_l/C_d), a blade profile was chosen as the most efficient one for mine ventilation fans.
Practical implications	This study forms a basis for selecting appropriate blade profiles for the axial flow fans used for ventilation in mining industry.
Originality/ value	The application of an appropriate aerofoil blade profile will impart energy efficiency to the mine ventilation fans and thereby result in energy saving in mine ventilation.

Keywords

mine ventilation, axial flow fan, energy efficiency, aerofoil, lift and drag, CFD

1. INTRODUCTION

Mine ventilation fans run 24 hours a day and throughout the year for maintaining a comfortable working environment for the miners working below ground. Mostly, conventional aluminium alloy bladed fans are used for underground mine ventilation, which are neither properly designed nor appropriately selected to suit the desired condition. As a result, the consumption of electricity during their operation constitutes the largest component of the operating cost for mine ventilation and accounts for one third of a typical underground mine's entire electrical power cost (Vergne, 2003). Belle (2008) has reported that the consumption of electricity by the main ventilation fan of a major mining company alone can be in the region of 120 MW. Therefore, ventilation is undoubtedly the most significant cost component of any underground

mine and a major part of this is made up by the main mine fans. The electric power consumption profile in Polish mines, reported by Krzystanek and Wasilewski (1995), revealed that the mine fans together with dewatering pumps and compressors that operate continuously consume over 40% of the total electrical energy consumption of the mines and out of which 14% is consumed by the main fans itself.

In this energy crunch world, the mining industry is facing the challenges of increasing energy costs. Therefore, investigations are ongoing and more focus is being given to reducing energy consumption in the ventilation systems. Enhancing energy efficiency is one of the alternatives for minimizing energy consumption in any system. In mine ventilation, energy consumption can be reduced by improving efficiency with the suitable design of ventilation fans. The design and selection of the ventilation fans are of foremost importance with

regards to operation and energy consumption. Furthermore, improvement in overall ventilation system efficiency can be achieved by reducing wasteful air power and enhancing fan efficiency. It is obvious that the power consumption will be less if the fan efficiency is more and vice versa (Sharma, 2002). The power consumption in fans depends to a large extent on the various losses involved, viz. impeller friction loss, entry loss, shock loss, clearance loss and diffuser loss, and the high losses in fans which are attributed to poor designs (Eck, 1973). Sen (1997) observed that the excess power consumption in axial flow main mine ventilation fan occurs because of the unrefined design approach, careless selection and incorrect installation of the fan. According to Sen (1997), a combination of aerodynamic, mechanical, electrical, structural and operational factors are involved in any overall optimization exercise, i.e. attainment of high fan efficiency or minimum power consumption. According to Hustrulid and Bullock (2001), the main reasons for very poor efficiency of old design colliery fans are due to poor aerodynamic design, improper fan selection and poor aerodynamics at the fan site, which are the root causes that yield static efficiencies below 50%. Therefore, enhancing energy efficiency in mine fans by minimizing various losses is an important facet of energy saving and it is mainly governed by proper design of the ventilation fans. The design of fan blades constitutes the most significant feature of the fans. Belle (2008) has reported that a 10% increase in main fan efficiency with a 10% reduction in electricity consumption may result in a saving of 10.81 MW of electricity per annum; this would have a net present benefit of US$ 16.08 million over 10 years. Several other approaches, viz. use of fan blades made of composite material such as FRP (fibreglass reinforced plastic), application of variable speed drives and the ventilation-on-demand (VOD) concept have also been tried in order to reduce energy consumption in ventilation fans (Mishra, 2004; Panigrahi, Mishra, Divaker, & Sibal, 2009).

The shape of the blades, which are of aerofoil sections in the case of axial flow fans, plays an important role in the performance of the fans and fan efficiency is greatly dependent on the profile of the blades. Therefore, there is a scope for improving energy efficiency by reducing losses and enhancing the efficiency of fans by using aerodynamically designed fan blades made of suitable material. From this point of view, the design of mine fan blade profiles with suitable aerofoil section is very much desired. Nowadays, computational fluid dynamics (CFD) is widely used in the field of aerodynamics for design and analysis of aerospace vehicles. Simulation of airflow around the aerofoil sections using CFD has been studied by several researchers (Kieffer, Moujaes & Armbya, 2006; Eleni, Athanasios, & Dionissios, 2012; Rajakumar & Ravindran, 2012; Bai, Sun, Lin, Kennedy, & Williams, 2012). Rumsey and Ying (2002) reported CFD capability in predicting surface pressures, skin friction, lift, and drag with reasonably good accuracy at angles of attack below stall in high-lift flow fields.

Keeping this in mind and with a broader aim of reducing energy consumption in mine ventilation fans, numerical simulations of the aerodynamic effects of different angles of attack on the selected aerofoil sections have been carried out in this study in a turbulent Reynolds number flow using the k-ε turbulence model. The aerodynamic characteristics of the

aerofoil sections viz. lift and drag coefficients at various angles of attack are determined for selecting a suitable profile for the axial flow mine ventilation fan blades giving the highest lift to drag ratio.

2. GENERAL AERODYNAMICS OF AXIAL FLOW FANS

A fan is simply a machine which develops the pressure necessary to produce the required airflow rate and overcome flow resistance of the system by means of a rotating impeller using centrifugal or propeller action, or both. The axial flow fans are commonly used in mine ventilation in lieu of centrifugal fans due to high efficiency, compactness, non-overloading characteristics, development of adequate pressure, etc. (Misra, 2002). The axial flow fan in its simplest form as diagrammatically shown in Figure 1 incorporates a rotor, which consists of a hub fitted with aerofoil section blades in a radial direction. The blades or vanes which constitute the main component of axial flow fan are the surfaces that work by means of dynamic reaction on the air and develop positive air pressure during their rotation due to the development of lift force. The forces acting on a typical aerofoil section of an axial flow fan blade are shown in Figure 2. The lifting force acts at right angles to the air stream and the dragging force acts in the same direction of the air stream and is responsible for losses due to skin friction.
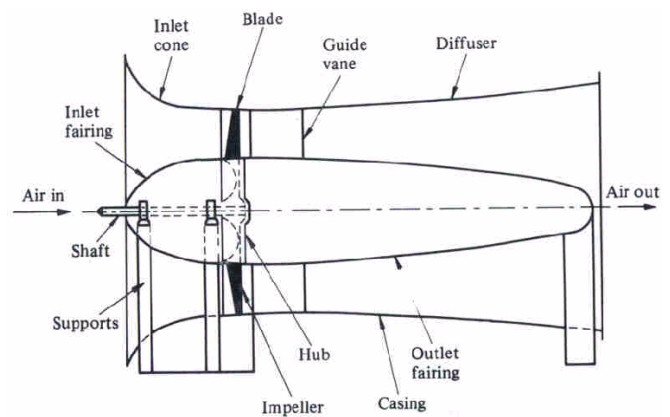

Fig. 1. The schematic of axial flow fan (Vutukuri & Lama, 1986)
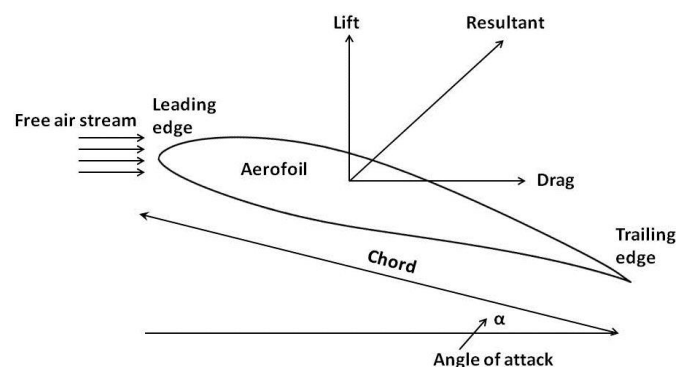

Fig. 2. Forces acting on a typical aerofoil section of axial flow fan blade

The efficiency of axial flow fans is greatly dependent on the profile of the blade, and the aerodynamic characteristics of the fan blades are strongly affected by the shape of the blade cross section. The cross section of fan blades is of

a streamlined asymmetrical shape, called the blade's aerodynamic profile and is decisive when it comes to blade performance. Even minor alterations in the shape of the profile can greatly alter the power curve and noise level. Therefore, it is essential to choose an appropriate shape with great care, in order to obtain maximum aerodynamic efficiency. An aerodynamic profile with optimum twist, taper and higher lift-drag ratio can provide total efficiency as high as 85–92%. The axial flow fan blades are of aerofoil sections and the idea behind using aerofoil blades is to maintain the proper streamlining of air to reduce losses caused due to form drag as well as from strength considerations (Misra, 2002). The blade performance characteristics may be predicted from the aerodynamic characteristics such as lift and drag coefficients of the chosen aerofoil section and given by the following equations:

$$C_l = \frac{L}{\frac{1}{2}\rho V^2 A} \qquad (1)$$

$$C_d = \frac{D}{\frac{1}{2}\rho V^2 A} \qquad (2)$$

where C_l is the coefficient of lift, C_d is the coefficient of drag, L is the lift force, D is the drag force, ρ is the density of air, V is the velocity of undisturbed airflow and A is the blade reference area.

The aerodynamic lifting force is a vital component and must be much greater than the drag component. Since lift contributes to the head generated by the fan and the drag causes loss due to skin friction in the wake behind the vane, the profile offering higher L/D ratio is considered more efficient (Misra, 2002). Maximum lift to drag provides a combinatory measure of the performance of the aerofoil and, therefore, the C_l/C_d curve can be likened to the efficiency characteristic of a fan. In the case of mine ventilation fans, an aerofoil profile generating high lift coefficient and offering high lift to drag ratio is needed for minimizing losses, producing high head and improving the efficiency of the fan provided it fulfils the other constraints like economy, change in mine resistance over time and other factors. These requirements are better fulfilled by the non-symmetrical aerofoils and are, therefore, commonly preferred for fan blades than symmetrical ones.

The lift and profile drag of the aerofoil shaped blades, when move through air, vary with the structure of the aerofoil and variations in the angle of attack (α). The angle of attack is the angle between the velocity vector and the chord line of the aerofoil (Figure 2). As the angle of attack increases, the coefficient of lift increases in a near-linear manner. However, at an angle of attack usually between 12 and 18°, breakaway of the boundary layer occurs on the upper surface. This causes a sudden loss of lift and an increase in drag, known as stall condition. In this condition, the formation and propagation of turbulent vortices causes the fan to vibrate excessively and to produce additional low frequency noise (McPherson, 1983).

The aerodynamic design of axial flow fans is a very complex process and mainly consists of designing two-dimensional blade sections at various radii. Over the past few decades, lots of effort has been put in to aerodynamic improvements of mine fans. Advances in aerodynamic design, which incorporate aerofoil section blading with lower aspect ratios, higher solidities and higher stagger angles have led to an increase in static-pressure rise. In addition to aerodynamic improvements, the use of improved materials and advanced mechanical design techniques also had a significant contribution. In conventional aluminium alloy bladed mine fans, their cross section barely matches a suitable aerofoil geometry that can develop sufficient lift and minimal drag forces. Moreover, the roughness of the blade surface considerably increases the losses. As a result, they may not reach the desired efficiency and cause a loss of energy. Eckert (1953) found that unmachined cast-iron blades give an efficiency ~10% lower than machined blades. Hence, careful smoothening of the blade surfaces is essential to obtain better fan efficiency.

3. CFD ANALYSIS OF THE AEROFOIL SECTIONS

In this study, the CFD package ANSYS Fluent 6.3.26 is used to perform the numerical simulation of airflow around the selected aerofoil sections. Fluent solvers are based on the finite volume method in which the domain is discretized into a finite set of control volumes (or cells). It solves conservation equations for mass and momentum to determine the pressure distribution and therefore fluid dynamic forces acting on the wing as a function of time. Six aerofoil sections, viz. EPPLER 420, EPPLER 544, EPPLER 855, FX 74 CL5 140, NACA 747A315 and NACA 64(3)-418 have been chosen based on an extensive literature review for 2-D simulation to select a suitable aifoil section for the blades of axial flow mine ventilation fans. Most of these aerofoils are used in aeroplanes, wind turbines, high velocity rotors, sailplanes and rotorcrafts etc.

3.1. Geometry creation and meshing

The aerofoil geometries of the chosen aerofoils have been created with the coordinates obtained from the airfoil coordinates database (http://www.ae.illinois.edu/m-selig/ads/coord_database.html) and shown in Figures 3.

Gambit 2.4.6, the pre-processor of Fluent 6.3.26 is used to create the discretized domain or mesh with a far-field and near-field area and exported to Fluent for analysis. Computational domain or the far-field distance, which is about 15 times the size of that of the chord length surrounding the centrally located aerofoil, is created for each profile. The domain boundary is set as a pressure-far-field and the surface of the aerofoil is set as wall. The meshing is done based on two-dimensional structured C-grid topology in x-y direction giving rise to average quadrilateral cells of about 160000 for all of the aerofoils. Figure 4 shows the meshed flow domain surrounding an aerofoil. The resolution of the mesh close to the aerofoil region is made greater for better computational accuracy. The height of the first cell adjacent to the surface of the aerofoils is set to 10^{-5}, corresponding to a maximum y^+ of approximately 0.2.
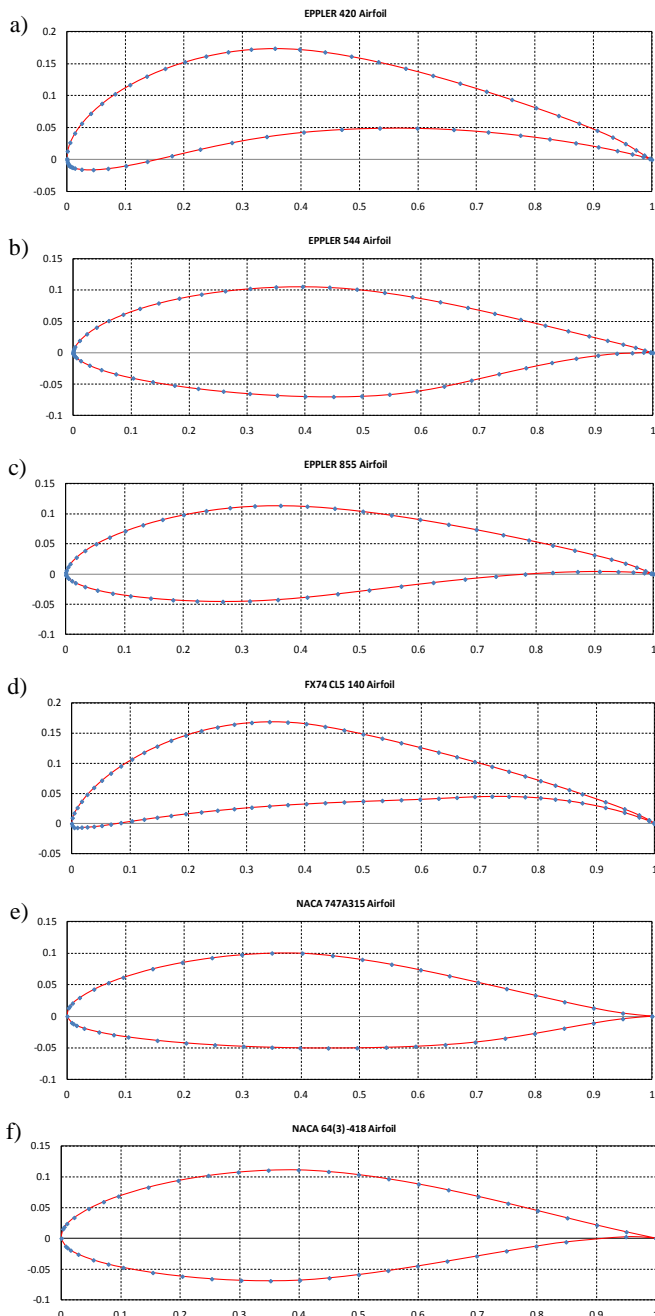
a)

EPPLER 420 Airfoil

b)

EPPLER 544 Airfoil

c)

EPPLER 855 Airfoil

d)

FX74 CL5 140 Airfoil

e)

NACA 747A315 Airfoil

f)

NACA 64(3) -418 Airfoil

Fig. 3. The aerofoil geometries: a – EPPLER 420, b – EPPLER 544, c – EPPLER 855, d – FX 74 CL5 140, e – NACA 747A315 and f – NACA 64(3)-418

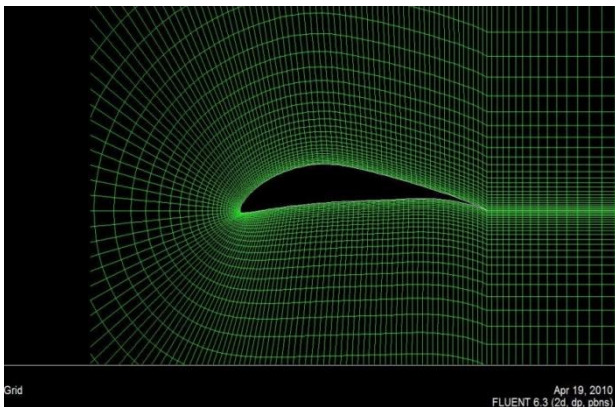### 3.2. CFD analysis for determination of lift and drag coefficients

The aerofoils with meshed flow domain are solved with Fluent solver for determining the lift and drag coefficients giving various input parameters, such as airflow direction, flow velocity (15 m/s), air density (1.225 kg/m^3), angle of attack, boundary conditions etc. The free air stream temperature is considered as 300 K, which is same as the environment temperature and at this given temperature, the density and viscosity of the air is ρ = 1.225 kg/m^3 and μ = 1.7894 × 10^{-5} kg/ms respectively. The flow is assumed to be incompressible. At this stage it is important to mention that the accuracy of CFD-based lift and drag prediction depends on the geometry representation, mesh size, flow solver, convergence level, transition prediction and turbulence model (Oskam & Sloo, 1998). For the numerical modelling of fluid-structure interaction problems, the choice of turbulence model is important. In this study the most widely used k-ε turbulence model is chosen for simulation due to its simplicity (Kieffer et al., 2006; Hoo, Do, & Pan, 2005). This model, proposed by Launder and Spalding (1974), includes standard renormalization-group (RNG) and realizable models. The Reynolds number for the simulations is considered as Re = 3 × 10^6. The angles of attack (AoA) are varied from 0 to 21° at 3° intervals for all the aerofoils. Additionally, the coefficients of lift (C_l) and drag (C_d) are determined at different angles of attack. Thereafter, the graphs of lift and drag coefficients versus angle of attack are plotted and the AoA corresponding to the maximum lift to drag ratio is determined. The pressure and velocity contours surrounding the aerofoil sections are also generated at the angle of attack which produces maximum lift to drag ratio for analysing the variation in air velocity and pressure around the aerofoil.

4. RESULTS AND DISCUSSION

The static pressure and velocity plots showing the magnitude of the static pressure and air velocity in the flow field are obtained from the CFD simulation. The velocity and pressure distributions for all the aerofoils follow a similar pattern for all angles of attack. For instance, the contours of static pressure and velocity vector which are coloured according to velocity magnitude across the aerofoil EPPLER 420 at a particular angle of attack (AoA) are presented in Figures 5 through 8.
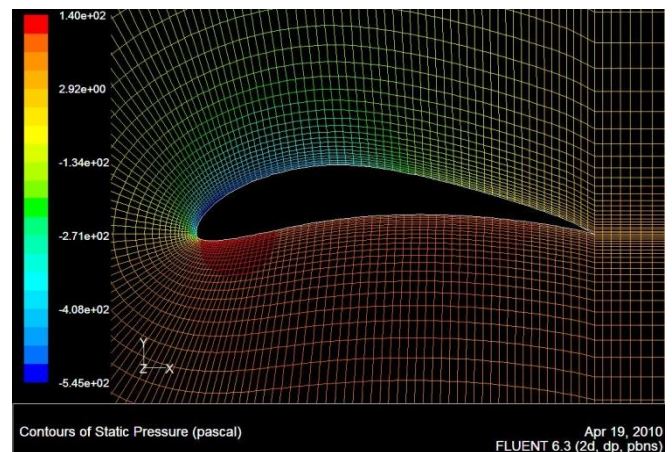

Fig. 4. The meshed flow domain surrounding aerofoil FX 74 CL5 140

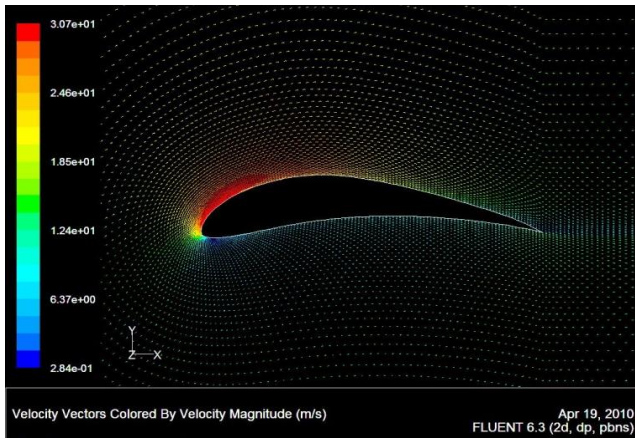**Fig. 5.** Contours of static pressure across aerofoil EPPLER 420

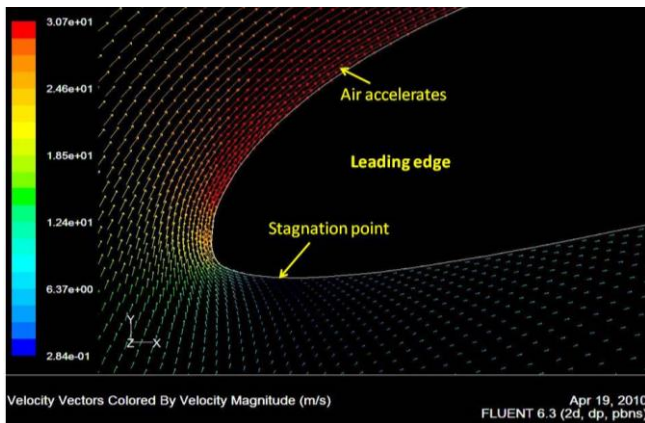**Fig. 6.** Velocity vectors coloured by velocity magnitude across aerofoil EPPLER 420

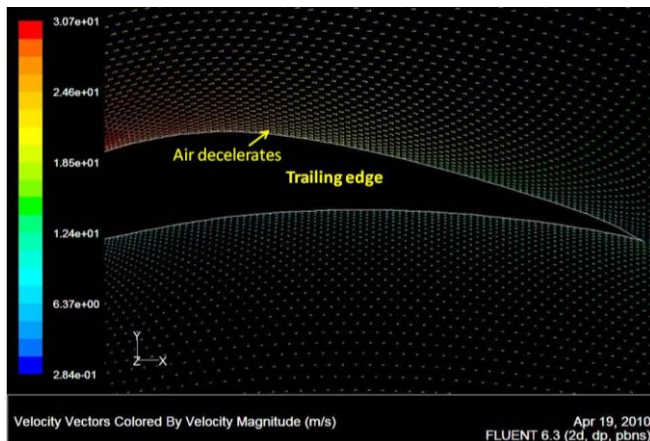**Fig. 7.** Velocity vectors coloured by velocity magnitude at the leading edge of aerofoil EPPLER 420

Fig. 8. Velocity vectors coloured by velocity magnitude at the trailing edge of aerofoil EPPLER 420

As expected from the normal aerofoils, the static pressure contours show that the pressure is negative on the upper surface and positive on the lower surface of the aerofoil, which is marked by a higher air velocity on the upper surface and lower velocity on the lower surface. The higher static pressure at the lower surface of the aerofoil effectively pushes the aerofoil upwards and is responsible for the generation of lift force, which acts perpendicularly to the inflowing airstream. The variation in velocity, which is caused due to the curvature of the aerofoil sections, can be clearly observed from the

contours of velocity vectors which is coloured according to velocity magnitude. This phenomenon complies with Bernoulli's equation. The air accelerates on the upper surface, as marked by an increase in the velocity magnitude and intensity of the colours of the velocity vectors. The reverse case is observed on the trailing edge of the aerofoil, i.e. the flow on the upper surface decelerates and converges with the flow on the lower surface. On the leading edge of the aerofoil (Figure 7), a stagnation point can be seen where the velocity of flow is nearly zero.

The variation of aerodynamic coefficients, i.e. the coefficients of lift (C_l) and drag (C_d) with angles of attack for all the aerofoil sections obtained from the CFD analysis are shown in Figure 9. The figure clearly shows that the lift and drag coefficients increase steadily with angles of attack. The coefficient of lift attains its maximum value at 12° AoA for airfoils EPPLER 855, FX 74 CL5 140 and NACA 64(3)-418, while it reachers its maximum of 15° for airfoils EPPLER 420, EPPLER 544 and NACA 747A315. Beyond these angles, the coefficient of lift decreases and the coefficient of drag decreases or remains relatively constant. At these AoAs, flow separation at the upper surface of the aerofoil sections can be observed. This indicates that the aerofoils begin to approach the "stall condition".
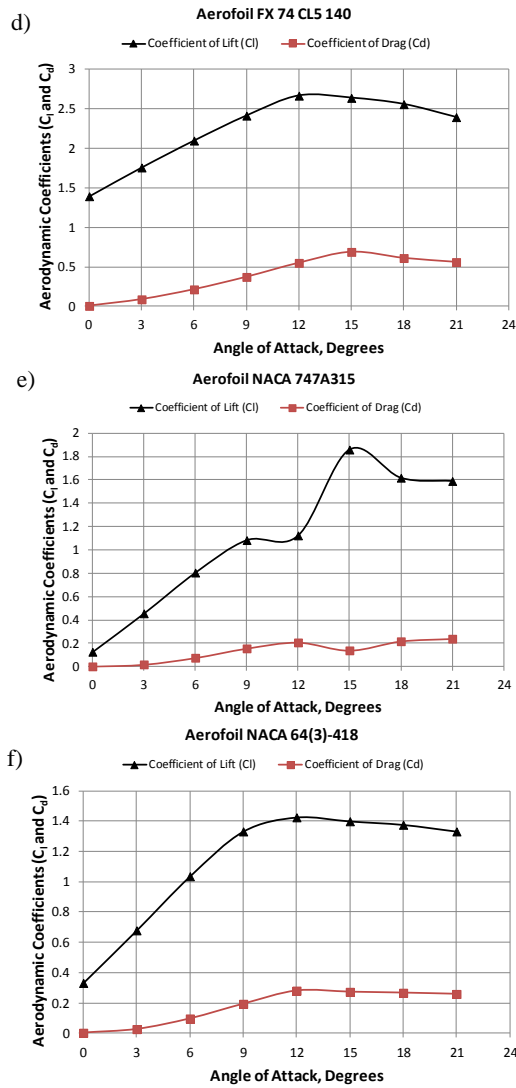
d)

e)

f)
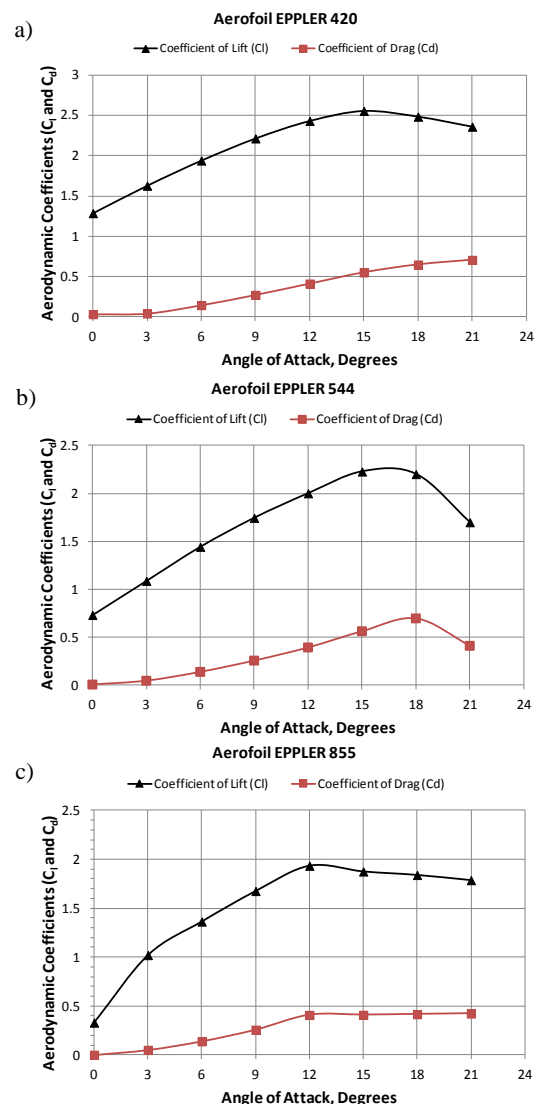
Fig. 9. Aerodynamic coefficients vs. angle of attack for the aerofoils
a – EPPLER 420, b – EPPLER 544, c – EPPLER 855, d – FX 74 CL5 140,
e – NACA 747A315 and f – NACA 64(3)-418

Table 1 summarizes the maximum C_l offered by the aerofoil sections and their corresponding angle of attack values. In addition, the C_d corresponding to the maximum C_l and the C_l/C_d ratios, a measure used for prediction of efficiency of the aerofoil sections are presented in the table. The results indicate that the maximum C_l, which varies in the range of 1.425–2.667 is obtained at AoAs ranging from 12 to 15 degrees in most of the aerofoil sections. Thereafter, the C_l falls and the region of high velocity begins to separate from the aerofoil surface at the trailing edge, giving rise to the "stall condition". Aerofoil FX-74 L5 40 offers its highest C_l of 2.667 at AoA of 12°. It can also be noticed that, comparatively, NACA aerofoils offer a higher lift to drag ratio than the EPPLER aerofoils. Although the aerofoil NACA 747A315 offered a lower C_l value of 1.858, due to the least corresponding drag value of 0.1394, the C_l/C_d ratio, i.e. 13.329 happens to be the highest amongst all the aerofoils analyzed in this study. This indicates that the aerofoil NACA 747A315 offers the least resistance to the airflow and can provide better efficiency to the fans. Therefore, the NACA 747A315 aerofoil section is the final choice for the fan blades.

Table 1. Summarized CFD analysis results of the aerofoil sections

Profile ID	Angle of Attack (Degrees)	Max. C_l	Corresponding C_d	C_l/C_d ratio
E-420	15	2.553	0.551	4.633
E-544	15	2.228	0.563	3.957
E-855	12	1.934	0.408	4.740
FX-74 L5 40	12	2.667	0.549	4.858
NACA 747A315	15	1.858	0.139	13.367
NACA 64(3)418	12	1.425	0.281	5.071

5. CONCLUSIONS

Minimizing various losses involved in fan system can improve efficiency, which in turn facilitate savings in energy consumption. Fan efficiency is greatly dependent on the profile of the blade. The lift to drag ratio is a measure of the aerodynamic efficiency of the fan blade and an aerofoil with higher lift to drag ratio is considered as the most efficient one. This study presents CFD simulations of drag and lift coefficients of six different airfoils using the ANSYS Fluent software, which is a finite volume based commercial code, to help with the selection of an energy-efficient blade profile for mine ventilation fans. In this study, six different airfoil sections are considered for CFD simulations to study the effect of the variation of angle of attack on the aerodynamic coefficients. The results indicate that NACA aerofoils offer a higher lift to drag ratio and the aerofoil NACA 747A315 offers the highest C_l/C_d ratio of all at 13.329. Therefore, if the blades of axial-flow mine ventilation fans are made of NACA 747A315 aerofoil section, it can provide better efficiency to the fans and help in minimizing energy consumption.

References
Bai, Y., Sun, D., Lin, J., Williams, F., & Kennedy, D. (2012). Numerical aerodynamic simulations of a NACA airfoil using CFD with block-iterative coupling and turbulence modelling. *International Journal of Computational Fluid Dynamics*, 26(2), 119–132.

Belle, B.K. (2008). Energy savings on mine ventilation fans using "Quick-Win" Hermit Crab Technology-A perspective. In Jr. K.G. Wallace (Ed.), *12th U.S./North American Mine Ventilation Symposium* (pp. 427–433). Reno: The University of Nevada.

Eck, B. (1973). *Fans; design and operation of centrifugal, axial flow, and cross-flow fans*. Oxford: Pergamon Press.

Eckert, B. (1953). *Axial Kompressoren und Radial Kompressoren*. Berlin: Springer Verlag.

Eleni, D.C., Athanasios, T.I., & Dionissios, M.P. (2012). Evaluation of the turbulence models for the simulation of the flow over a National Advisory Committee for Aeronautics (NACA) 0012 airfoil. *Journal Mechanical Engineering Research*, 4(3), 100–111.

Hoo, E., Do, K.D., & Pan, J. (2005). An investigation on the lift force of a wing pitching in dynamic stall for a comfort control vessel. *Journal of Fluids and Structure*, 21, 707–730. Retrieved from http:// www.ae.illinois.edu/m-selig/ads/coord_database.html. Accessed on 18.05.2011.

Hustrulid, W.A., & Bullock, R.L. (2001). *Underground mining methods: engineering fundamentals and international case studies*. Englewood, CO: Society for Mining, Metallurgy and Exploration.

Kieffer, W., Moujaes, S., & Armbya, N. (2006). CFD study of section characteristics of Formula Mazda race car wings. *Mathematical and Computer Modelling*, 43, 1275–1287.

Krzystanek, Z., & Wasilewski, S. (1995). Monitoring and control of main fans for minimization of power consumption. In A.M. Wala (Ed.), *Proceedings of the 7th US Mine Ventilation Symposium* (pp. 75–81). Littleton, CO: Society for Mining, Metallurgy, and Exploration.

Launder, B.E., & Spalding, D.B. (1974). The numerical computation of turbulent flows. *Computer Methods in Applied Mechanics and Engineering*, *3*(2), 269–289.

McPherson, M.J. (1983). *Subsurface Ventilation and Environmental Engineering*. Netherlands: Kluwer Academic Publishers.

Mishra, D.P. (2004). *A Study of Energy Consumption Profile of Main Mine Ventilation Fans and Development of a Technique to Reduce the Energy Requirement in Such Systems*. Dissertation. Dhanbad: Indian School of Mines.

Misra, G.B. (2002). *Mine Environment and Ventilation*. New Delhi: Oxford University Press.

Oskam, B., & Sloof, J.W. (1998). Recent advances in computational aerodynamics at NLR. *AIAA* Paper 98-0138. doi: 10.2514/6. 1998-138.

Panigrahi, D.C., Mishra, D.P., Divaker, C., & Sibal, S.J. (2009). Application of fibreglass reinforced plastic blades in main mine ventilation fans: an innovative concept of energy saving. In D.C. Panigrahi (Ed.), *Mine Ventilation* (pp. 709–715). New Delhi: Oxford & IBH Publishing Co. Pvt. Ltd.

Rajakumar, S., & Ravindran, D. (2012). Iterative approach for optimising coefficient of power, coefficient of lift and drag of wind turbine rotor. *Renewable Energy*, *38*(1), 83–93.

Rumseya, C.L., & Ying, S.X. (2002). Prediction of high lift: review of present CFD capability. *Progress in Aerospace Sciences*, *38*(2), 145–180.

Sen, P.K. (1997). Reducing power consumption for axial flow mine ventilation fans. *Journal of Mines, Metals and Fuels*, *45*(9–10), 301–303.

Sharma, R.N. (2002). Economics of mine ventilation. In *Proceedings of International Conference on Mineral Industry: Issues on Economics, Environment and Technology* (pp. 75–87). India: The Mining, Geological and Metallurgical Institute of India.

Vergne, J.N.D.L. (2003). *The Hard Rock Miner's Handbook*. North Bay, ON: McIntosh Engineering Limited.

Vutukuri, V.S., & Lama, R.D. (1986). *Environmental Engineering in Mines*. Cambridge: Cambridge University Press.